Journal of Basic and Applied Engineering Research
p-ISSN: 2350-0077; e-ISSN: 2350-0255; Volume 4, Issue 2; January-March, 2017, pp. 123-127

http://www.krishisanskriti.org/Publication.html

Computational Analysis of Subsonic Circular Jet and Bevel Nozzle

Arthur John B[1] and George Johny[2]

[1]Government Engineering College Thrissur
[2]VTU Center for PG Studies Mysore
E-mail: [1]arthurarjohn@gmail.com, [2]georgejohny332@gmail.com

Abstract—*Jet aerodynamics is highly dependent on the fluctuating quantities in a flow and determination of these quantities experimentally is very expensive and time consuming. The flow fluctuations associated with turbulence give rise to additional transfer of momentum, heat and mass. In the present work numerical simulations of a turbulent compressible subsonic isothermal circular jet and bevel nozzle of 50mm diameter and Mach number 0.75 using RANS is carried out. A heated bevel nozzle, where jet exit temperature T_j is twice that of free stream temperature T_∞ is compared with an isothermal bevel nozzle. Simulations are performed in a three dimensional computational domain and the turbulence model used is SST k-ω. The flow is investigated for axial and radial profiles of velocity components and all the turbulent characteristics. The results are found agreeable with the available results from referred journals. In this work, modelling and meshing are done in GAMBIT and the simulations using FLUENT*

Keywords*: RANS, Subsonic, Turbulence model, Mach number, Simulation*

1. INTRODUCTION

Theoretical analysis and prediction of turbulence has been, and to this date still is, the fundamental problem of fluid dynamics, particularly of computational fluid dynamics (CFD). The major difficulty arises from the random or chaotic nature of turbulence phenomena. Because of this unpredictability, it has been customary to work with the time averaged forms of the governing equations, which inevitably results in terms involving higher order correlations of fluctuating quantities of flow variables.

All flows in engineering practices, simple ones such as two-dimensional jets, wakes, pipes flows and more complicated three-dimensional ones, become unstable above a certain Reynolds number (UL/v). At low Reynolds number flows are laminar. At higher Reynolds number flows are observed to become turbulent. A chaotic and random state of motion develops in which the velocity and pressure change continuously with time within substantial regions of flow. The velocity fluctuations are found to give rise to additional stresses on the fluid, so called Reynolds stresses.

Turbulent flows possess irregularity or randomness. A full deterministic approach is very difficult. Turbulent flows are usually described statistically. Turbulent flows are always chaotic. But not all chaotic flows are turbulent. Turbulent flows are rotational; that is, they have non-zero vorticity. Mechanisms such as the stretching of three-dimensional vortices play a key role in turbulence. The diffusivity of turbulence causes rapid mixing and increased rates of momentum, heat, and mass transfer. A flow that looks random but does not exhibit the spreading of velocity fluctuations through the surrounding fluid is not turbulent. If a flow is chaotic, but not diffusive, it is not turbulent. Turbulent flows are dissipative. Kinetic energy gets converted into heat due to viscous shear stresses. Turbulent flows die out quickly when no energy is supplied. Random motions that have insignificant viscous losses, such as random sound waves, are not turbulent.

An LES or DNS can be used to obtain the non-linear near-field, which in the jet noise case corresponds to the hydrodynamic jet region. Freund [5] investigated sources of sound in a Mach 0.9 jet at a Reynolds number of $Re_D = 3.6 \times 10^3$ using DNS. Bogey and Bailly[2][4] investigated the effects of inflow conditions on the flow field and the radiated sound of high-Reynolds-number, $Re_D = 4.0 \times 10^5$, Mach 0.9 jet.

In DNS, all scales of the turbulent flow field are computed accurately, which requires a mesh fine enough to capture even the smallest scales in the flow, whereas in LES, only the large scales of the flow are resolved and the influence on these large scales of the smaller, unresolved scales is modelled using a subgrid scale model. With the computational resources available today, DNS is restricted to fairly simple geometries and low Reynolds number flows. Moreover, it is believed, Mankbadi et al [3] that large scales are more efficient than small ones in generating sound, which justifies the use of LES for sound predictions. Another approach is to use a less computationally expensive RANS calculation to obtain a time-averaged flow field. Information about length and time scales in the time-averaged flow field can then be used to synthesis turbulence in noise source regions.-This method is promising since simulations of high Reynolds number flows are possible

with reasonable computational efforts. In contrast to a RANS calculation, where all turbulent scales in the flow are modelled and only a time-averaged flow field is obtained, DNS and LES directly provide information about turbulent quantities and sources of noise. Since sound predictions are not considered it will be fine to investigate turbulence characteristics using RANS. This is the objective of present work.

2. MODELLING

In the present study a RANS of a Mach 0.75 nozzle/jet configuration has been performed. The Reynolds number based on the nozzle exit diameter and the jet velocity at the nozzle exit plane, ReD, was 5.0 *10^4. An isothermal jet is simulated, i.e. the static temperature in the nozzle exit plane, T_j, is equal to the static temperature of the ambient air, T∞. The table below show the flow properties. The geometry was created in gambit and was simulated in fluent.

The geometry of 3dimensional circular jet was created in gambit and simulations were conducted in fluent. Simulations were performed on mesh containing 4, 27,940 nodes.

Table 1: Flow Properties

Properties	Jet
U_i / C	0.75
T_i / T_∞	1.0
P (pa)	101325
ρ (kg/m^3)	1.225561
C (m/s)	340.174
U (m/s)	0.0
T (K)	288
T_{0i} (K)	320.4
Re D	5*10^4

Fig. 1 gives an overview of computational set up used Anderson et al [1]. In order to minimize the effect of reflections at the domain outlet of the predicted flow field, a damping zone was added at the domain outlet. The axial extent of the physical part of the domain downstream of the nozzle exit is 2.5 meters, which is equal to 50 nozzle diameters (D_j = 50mm). The radial exit is 10 Dj at the nozzle exit plane and 20 Dj at the domain outlet.

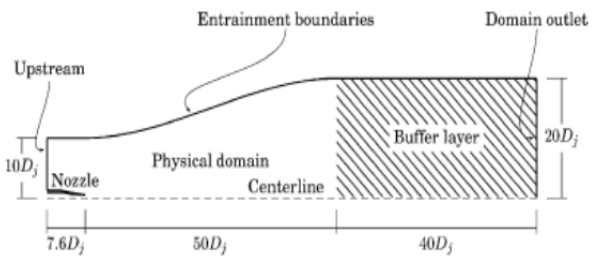

Fig. 1: Computational domain [N.Anderson et.al]

Stagnation conditions were specified at the nozzle inlet and static conditions, equal to ambient conditions were specified at all other places.

3. GOVERNING EQUATIONS

The turbulent flow equations for compressible flows are shown below. The extra turbulent stresses that appear on Reynolds equation are called Reynolds stresses. The normal stresses involve. The respective variances of the x, y and z velocity. They are always non-zero because they contain squared velocity fluctuations. The shear stresses contain second moments associated with correlations between different velocity components.

Continuity

$$\frac{\partial \rho}{\partial t} + div(\rho \mathbf{U}) = 0$$

Reynolds equations

$$\frac{\partial(\rho U)}{\partial t} + div(\rho U \mathbf{U}) = -\frac{\partial P}{\partial x} + div(\mu\ grad\ U) + \left[-\frac{\partial\left(\rho\overline{u'^2}\right)}{\partial x} - \frac{\partial(\rho\overline{u'v'})}{\partial y} - \frac{\partial(\rho\overline{u'w'})}{\partial z}\right] + S_{Mx}$$

$$\frac{\partial(\rho V)}{\partial t} + div(\rho V \mathbf{U}) = -\frac{\partial P}{\partial y} + div(\mu\ grad\ V) + \left[-\frac{\partial(\rho\overline{u'v'})}{\partial x} - \frac{\partial\left(\rho\overline{v'^2}\right)}{\partial y} - \frac{\partial(\rho\overline{v'w'})}{\partial z}\right] + S_{My}$$

$$\frac{\partial(\rho W)}{\partial t} + div(\rho W \mathbf{U}) = -\frac{\partial P}{\partial z} + div(\mu\ grad\ W) + \left[-\frac{\partial(\rho\overline{u'w'})}{\partial x} - \frac{\partial(\rho\overline{v'w'})}{\partial y} - \frac{\partial\left(\rho\overline{w'^2}\right)}{\partial z}\right] + S_{Mz}$$

Scalar transport equation

$$\frac{\partial(\rho\Phi)}{\partial t} + div(\rho\Phi \mathbf{U}) = div(\Gamma_\Phi\ grad\ \Phi) + \left[-\frac{\partial(\rho\overline{u'\varphi'})}{\partial x} - \frac{\partial(\rho\overline{v'\varphi'})}{\partial y} - \frac{\partial(\rho\overline{w'\varphi'})}{\partial z}\right] + S_\Phi$$

4. RESULTS AND DISCUSSIONS

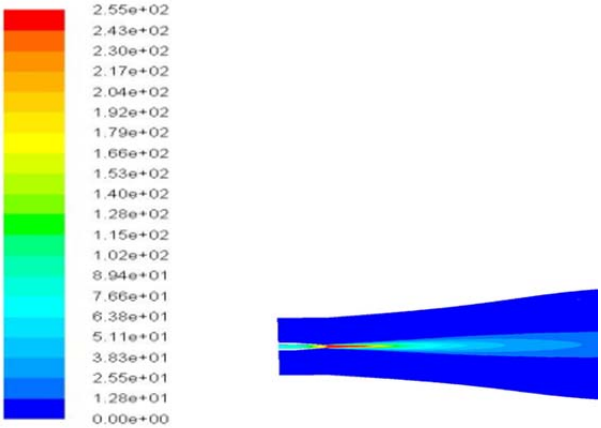

Fig. 2: Contours of axial velocity of isothermal circular jet

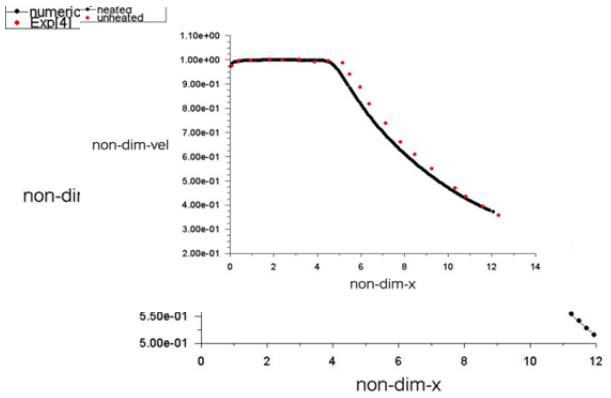

Fig. 3: Center line profiles of axial velocity of circular isothermal jet compared with experimental data [1]

The physics behind potential core is that when the jet spreading rate and mixing are higher the turbulence can be reached at a much faster rate i.e., the potential core becomes shorter. There is slight over prediction of experimental values with computed value, but it is acceptable.

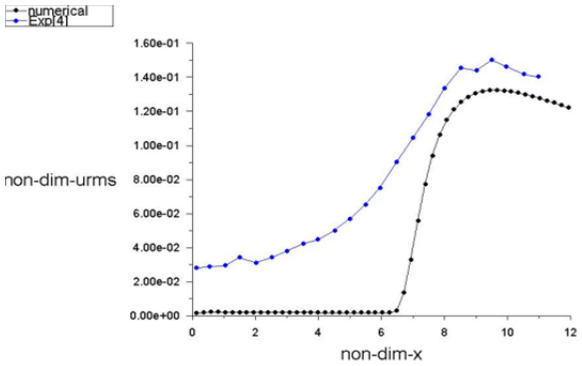

Fig. 4: Axial profiles of turbulent intensities of isothermal circular jet compared with experimental data [1] non dimensional Urms vs non dim x

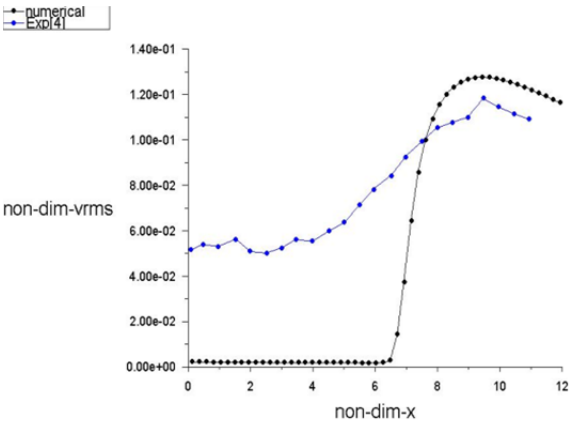

Fig. 5: Axial profiles of turbulent intensities of isothermal circular jet compared with experimental data [1] non dimensional Vrms vs non dim x

Figs. 4 and 5 indicate turbulent intensity plots for isothermal jet non dimensionaling Urms and Vrms with the non dimensionalized axial distance x. The computed values are compared with the experimental values [1].The differences in levels of Urms and Vrms indicate that the turbulence anisotropy is captured. The peak levels of predicted turbulence intensity are shifted toward the nozzle exit, which is consistent with the under prediction of potential core lengths because maximum turbulent intensity is found where the potential core closes. The reason for the difference in peak level can be probably attributed to the fact that the simulations are performed on RANS(Reynolds averaged Navier Stokes Equation) and experimental values are computed using LES (Large Eddy Simulation) which is computationally more accurate but time consuming and expensive.

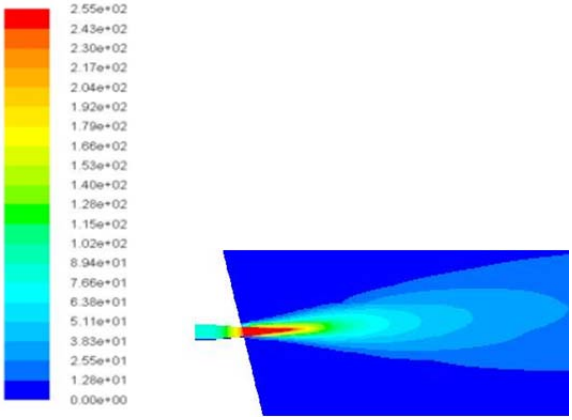

Fig. 6: Velocity contours of isothermal bevel nozzle

The region of potential core is very small in bevel due to better mixing.

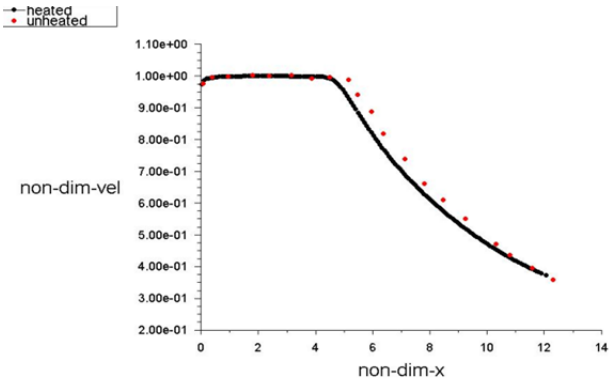

Fig. 7: Center line profiles of axial velocity. Computed values of heated bevel nozzle is compared with the computed values of isothermal bevel nozzle

Experiments have shown that increasing the temperature ratio T_j/T_∞ results in narrower jet [6]. Bevel has much shorter potential core due to enhanced jet spreading and mixing at the

initial region. Furthermore it has been observed that length of potential core decreases with increasing temperature ratio. By heating the potential core becomes shorter again. There is a very slight decrease in potential core upon heating. This could be probably due to the fact that bevel has already a shorter potential core. The jet seems to be narrow with increased velocity decay.

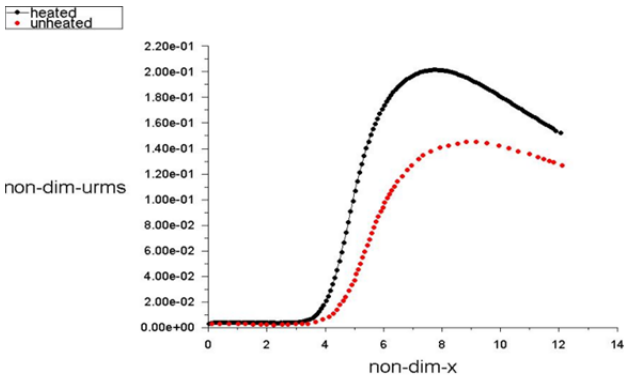

Fig. 8: Axial profiles of turbulent intensities isothermal vs heated bevel jet: Non-dim Urms vs Non dim-x

This plot is an indication of turbulence characteristics of bevel nozzle. The plot completely agrees with the theory that maximum turbulence is captured for heated jet due to better mixing, thus resulting in shorter potential core. Heating the jet results in narrow jet with shorter potential core thus reducing the transition period and turbulence can be achieved much earlier.

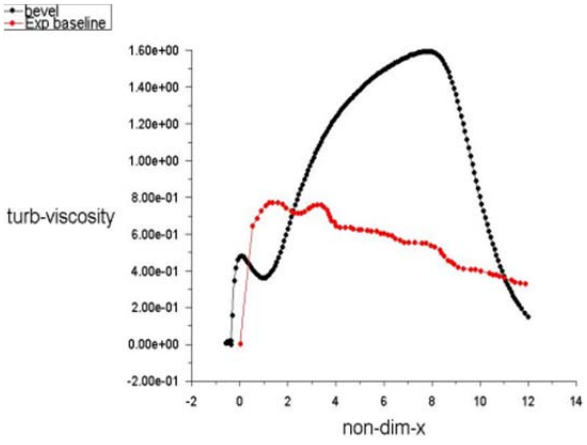

Fig. 9: Variation of turbulent viscosity for an isothermal bevel nozzle with experimental data [7]

This is contrary to the expectations that turbulent viscosity for bevel nozzle is maximum at some point downstream. The maximum is found at X/Dj =8, whereas turbulent viscosity is substantially lower in the region of X/Dj < 4.This is due the fact that bevel nozzle is a high penetration nozzle.

5. CONCLUSION

Computational analysis of subsonic jets of mach 0.75 is conducted for circular jet and bevel nozzle. The physics behind selecting these geometries are because of their distinct flow properties and turbulence characteristics. Circular jet has been compared to the experimental values [1] and yielded good agreement, although the peak of turbulent intensities captured are different. The differences in levels of U_{rms} and V_{rms} indicate that the turbulence anisotropy is captured. The peak levels of predicted turbulence intensity are shifted toward the nozzle exit, which is consistent with the under prediction of potential core lengths because maximum turbulent intensity is found where the potential core closes. This could also happen due to the fact that experimental data's are obtained from LES which is computationally more accurate and expensive, time consuming compared to RANS. According to the computational analysis bevel nozzle has the shortest potential core and thus improved jet spreading compared to circular geometry. Due to this fact, bevel has captured the highest turbulent intensity. Turbulent viscosity was investigated and it was found that contrary to theory bevel nozzle showed a lot of difference in peak compared to circular jet. The peak of turbulent viscosity for bevel shifts downstream, X/Dj =8 owing to the fact that bevel is a high penetration nozzle [7]. Heating the jet results in shorter potential core and enhanced mixing thus has a narrow jet. A comparison has been made for bevel nozzle under heated and isothermal conditions. Bevel already have a shorter potential core and after heating there is a slight reduction in potential core. A lot of work can be done in this area, since any modification at the nozzle exit results in enhanced jet spreading and better mixing.

There is lot of scope for future work in the area of computational fluid dynamics. A study on turbulence characteristics of non-circular jets can be carried out since the variation in geometry has a direct effect on flow as well as turbulence characteristics. Study on influence of chevrons of various taper angle on turbulence and flow properties are of greater interest since chevrons are high penetration nozzles which are having very distinct turbulent characteristics. Variation in turbulence characteristics and jet mixing for bevel nozzle of different nozzle exit angle can be made as an extension of present work. Many works have been carried out already but number of researches in the past decade in this field clearly mentions the vast opportunities in the field of computational dynamics.

REFERENCES"

[1] Niklas Andersson,Lars-Erik Eriksson, and Lars Davidson "Large-Eddy Simulation of Subsonic Turbulent Jets and Their Radiated Sound" University of Technology, SE-G¨oteborg, Sweden 2005,AIAA/CEAS 10th Aeroacoustics Conference, Manchester, England, United Kingdom

[2] Bogey, C. and Bailly, C., "LES of a High Reynolds, High Subsonic Jet: Effects of the Inflow Conditions on Flow and Noise". The 9th AIAA/CEAS Aeroacoustics Conference, No. 3170 in AIAA 2003, Hilton Head, South Carolina, 2003

[3] Freund, J., "Noise Sources in a Low-Reynolds-Number Turbulent Jet at Mach 0.9," *Journal of Fluid Mechanics*, Vol. 438, 2001, pp. 277–305.

[4] Mitchell, B., Lele, S., and Moin, P., "Direct Computation of the Sound Generated by Vortex Pairing in an Axisymmetric Jet," *Journal of Fluid Mechanics*, Vol. 383, 1999, pp. 113–142.

[5] Mankbadi, R., Shih, S., Hixon, R., and Povinelli, L., "Direct Computation of Jet Noise Produced by Large-Scale Axisymmetric Structures", J. Propulsion and Power, Vol. 16, No. 2, 2000, pp. 207.215.

[6] Hinze, J., "Turbulence", 2nd ed., McGraw–Hill, New York, 1975, Chap. 6.

[7] P.S. Tide, V. Babu, "Numerical predictions of noise due to subsonic jets from nozzles with and without chevrons" Applied Acoustics 70, 321–332, 2009